2015 IEEE Radio & Wireless Week

FINAL PROGRAM

Omni Hotel
San Diego, California, USA
25–28 January, 2015

RWW & RWS General Chair:
Karl Varian

General Co-Chair:
Sergio Pacheco, *Freescale*

RWW & RWS Technical Program Co-Chairs:
Jeremy Muldavin, *MIT Lincoln Laboratory*
Mehdi Shadaram, *University of Texas at San Antonio*

RWW & RWS Finance Chair:
Rashaunda Henderson, *University of Texas at Dallas*

WiSNet Conference Co-Chairs:
Alexander Koelpin, *University of Erlangen-Nuremberg*
Rahul Khanna, *Intel*

PAWR Conference Co-Chairs:
Almudena Suarez Rodriguez, *University of Cantabria*
Fred Schindler, *Qorvo*

BioWireleSS Conference Co-Chairs:
Katia Grenier, *LAAS-CNRS*
Syed Kamrul Islam, *University of Tennessee*

SiRF Conference Chair:
Chien-Nan Kuo, *National Chiao Tung University*

SiRF Technical Program Chair:
Julio Costa, *Qorvo*

SiRF Technical Program Co-Chair:
Hasan Sharifi, *HRL Laboratories*

RWS, PAWR, WiSNet, BioWireleSS Publications Chairs:
Wasif Tanveer Khan, Spyridon Pavlidis, Aida L. Vera Lopez *Georgia Institute of Technology*

SiRF Publication Chair:
Ming-Ta Yang, *Qualcomm*

2015 Radio & Wireless Week Sponsors:
IEEE Microwave Theory and Techniques Society (MTT-S)
IEEE Antennas and Propagation Society (APS)
IEEE Engineering in Medicine & Biology Society (EMBS)

http://www.radiowirelessweek.org

WEDNESDAY, 28 JANUARY 2015

WiSNet Session: WE1A

Insight in Sensor Networks and System Design

Chair: Rahul Khanna, Intel
Co-Chair: Andreas Stelzer, Johannes Kepler University, Linz

Room: Gallery 1

RWW Session: WE1B

Passive Components and Packaging I

Chair: Hualiang Zhang, University of North Texas
Co-Chair: Roberto Gomez-Garcia, University of Alcala

Room: Grand Salon A

SiRF Session: WE1C

Tunable and Reconfigurable Technologies

Chair: J.P. Raskin, Université catholique de Louvain (UCL)
Co-Chair:Monte Miller, Freescale

Room: Grand Salon B

BioWireleSS Session: WE1D

Micro Biosensing

Chair: Dietmar Kissinger , IHP GmbH
Co-Chair: JC Chiao, University of Texas Arlington

Room: Gallery 2

08:00

WE1A-1 Review of the Present Technologies Concurrently Contributing to the Implementation of the Internet of Things (IoT) Paradigm: RFID, Green Electronics, WPT and Energy Harvesting (Invited)

L. Roselli[1], C. Mariotti[1], P. Mezzanotte[1], F. Alimenti[1], G. Orecchini[1], M. Virili[1], N. B. Carvalho[2], [1]University of Perugia, Perugia, Italy, [2]University of Aveiro, Aveiro, United States

WE1B-1 Miniaturized Via-less Ultra-Wideband Bandpass Filter Based on CRLH-TL Unit Cell

A. O. Albursikan, M. Aqeeli, X. Huang, Z. Hu, The University of Manchester, Manchester, United Kingdom

WE1C-1 Reconfigurable Solutions for Mobile Device RF Front-ends (Invited)

A. Morris, wiSpry, San Diego, United States

WE1D-1 Why using High Frequency Dielectric Spectroscopy for Biological Analytics? (Invited)

M. Poupot[1,2], D. Dubuc[2,3], F. Artis[1,3], K. Grenier[2,3], J. Fournie[1,2], [1]CRCT , Av. Hubert Curien, France, [2]Univ. Toulouse [3], Toulouse, France, [3]CNRS, Toulouse, France

08:20

WE1A-2 Combined Localization and Data Transmissionin Energy-Constrained Wireless Sensor Networks

T. Nowsk[1], A. Koelpin[2], F. Dressler[3], M. Hartmann[1], L. Patino[1], J. Thielecke[1], [1]University of Erlangen-Nürnberg-Inst. Info. Tech., Erlangen, Germany, [2]University of Erlangen-Nürnberg-Inst. Elec. Eng., Erlangen, Germany, [3] University of Paderborn, Paderborn, Germany

WE1B-2 Dual-Band Negative Group Delay Circuit Using Defected Microstrip Structure

G. Chaudhary[1], P. Kim[1], J. Jeong[1], Y. Jeong[1], J. Lim[2], [1]Chonbuk National University, Jeonju-si, Republic of Korea, [2]Soonchunhyang University, Asan, Republic of Korea

08:40

WE1A-3 Wireless Integrated Sensor Nodes for Indoor Monitoring and Localization (Invited)

D. Kissinger[1,2], A. Schwarzmaier[2], F. Grimminger[4], J. Mena-Carrillo[4], W. Weber[4], G. Hofer[5], G. Fischer[3], R. Weigel[2], [1]IHP, Frankfurt (Oder), Germany, [2]Technische Universität Berlin, Berlin, Germany, [3]FAU Erlangen-Nuremberg, Erlangen, Germany, [4]Infineon Technologies, Neubiberg, Germany, [5]Infineon Technologies Austria, Graz, Austria

WE1B-3 A high power Ka-band SPST switch MMIC using 0.25 um GaN on SiC

S. Kaleem[1], J. Kuhn[2], R. Quay[2], M. Hein[1], [1]Ilmenau University of Technology, Ilmenau, Germany, [2]Fraunhofer Society for the Advancement of Applied Research, Freiburg, Germany

WE1C-2 An Integrated Reconfigurable Tuner in 45nm CMOS SOI Technology

A. Jou, C. Liu, S. Mohammadi, Purdue Universty, West Lafayette, United States

WE1D-2 Broadband Dielectric Characterization of CHO-K1 Cells Using Miniaturized Transmission-Line Sensor

N. Meyne[1], G. Fuge[2], S. Hemanth[2], H. K. Trieu[2], A. Zeng[2], A. F. Jacob[1], [1]Technische Universität Hamburg-Harburg-Inst. Hochfreq., Hamburg, Germany, [2]Technische Universität Hamburg-Harburg-Inst. Bioproz. und Biosys., Hamburg, Germany, [3]Technische Universität Hamburg-Harburg-Inst. Mikrosystem., Hamburg, Germany

09:00

WE1A-4 Low-Weight Wireless Sensor Network for Encounter Detection of Bats

M. Hierold[1], S. Ripperger[2], D. Josic[2], F. Mayer[2], R. Weigel[1], A. Koelpin[1], [1]University of Erlangen-Nuremberg, Erlangen, Germany, [2]Museum of Natural History, Berlin, Germany

WE1B-4 High Frequency-Selectivity Impedance Transformer

P. Kim[1], G. Chaudhary[1], J. Park[1], Y. Jeong[1], J. Lim[2], [1]Chonbuk National University, Jeonju, Republic of Korea, [2]Soonchunhyang University, Asan, Republic of Korea

WE1C-3 Ferroelectric MIM Capacitors for Compact High Tunable Filters

R. De Paolis[1], S. Payan[2], M. Maglione[2], G. Guegan[3], F. Coccetti[1], [1]CNRS, Toulouse, France, [2]CNRS, Bordeaux, France, [3]ST-Microelectronics, Tours, France

WE1D-3 A Microwave Sensor Dedicated to Dielectric Spectroscopy of Nanoliter Volumes of Liquid Medium and Flowing Particles

A. Landoulsi, C. Dalmay, A. Bessaudou, P. Blondy, A. Pothier, XLIM, Limoges, France

09:20

WE1A-5 Ad-Hoc Multilevel Wireless Sensor Networks for Distributed Microclimatic Diffused Monitoring in Precision Agriculture

A. Rodriguez de la Concepcion, R. Stefanelli, D. Trinchero, iXem Labs - Politecnico di Torino, Torino, Italy

WE1B-5 A Class of Planar Multi-Band Wilkinson-Type Power Divider with Intrinsic Filtering Functionality

R. Loeches-Sanchez[1,2], D. Psychogiou[2], D. Peroulis[2], R. Gomez-Garcia[1], [1]University of Alcala, Alcala de Henares, Spain, [2]Purdue University , West Lafayette, United States

WE1C-4 10.6 THz Figure-of-Merit Phase-change RF Switches with Embedded Micro-heater

J. Moon, H. Seo, D. Le, H. Fung, A. Schmitz, T. Oh, S. Kim, K. Son, B. Yang, HRL Laboratories, Malibu, United States

WE1D-4 Sub-microliter Microwave Dielectric Spectroscopy for Identification and Quantification of Carbohydrates in Aqueous Solution

F. Artis[1,2], D. Dubuc[1], J. Fournie[2], M. Poupot[2], K. Grenier[1], [1]LAAS-CNRS and Toulouse Univ., Toulouse, France, [2]CRCT, Toulouse, France

High Frequency-Selectivity Impedance Transformer

Phirun Kim[1], Girdhari Chaudhary[1], Junsik Park[1], Yongchae Jeong[1], and Jongsik Lim[2]

[1]Division of Electronics and Information Engineering, Chonbuk National University, South Korea,
[2]Department of Electrical Engineering, Soonchunhyang University, South Korea

Abstract —**This paper presents the design of an impedance transformer (IT) with high selectivity and wide out-of-band suppression characteristics. The proposed IT provides two transmission poles in the passband and a sharp frequency selective characteristic. For validation, a 50-to-20 Ω IT has been implemented at a center frequency (f_0) of 2.6 GHz. The measurement results show a return loss higher than 20 dB over the passband of 2.2-3 GHz and the insertion loss less than 0.4 dB over the same passband. The out-of-band suppression higher than 17 dB from DC to 1.85 GHz and higher that 11 dB from 3.5 GHz to 7.2 GHz are obtained.**

Index Terms — **Coupled line, impedance transformer, high selectivity, out-of-band.**

I. Introduction

The impedance transformer is widely used in RF circuits such power dividers/combiners [1], antenna [2], baluns [3], and power amplifiers [4]. The purpose of IT is to minimize reflections between two cascaded circuits of different terminated impedances and provide the maximum power transfer. The quarter-wavelength IT is mostly used in RF circuits due to simple implementation. However, most of the conventional ITs consider only passband impedance matching and ignore the out-of-band suppression characteristic. The out-of-band suppression characteristic of frequency selective RF circuits such as high power, high efficiency, and highly linear power amplifiers is one of important design issues.

Various studies have focused to design IT using coupled lines [5]-[6]. In [5], an open-circuited coupled line IT which can act as a DC block circuit was presented. Similarly a coupled line IT where the coupled port was connected back to the input port was presented in [6]. In [7] a dual transmission line with different lengths was used to design bandwidth controllable IT. Recently, strip-line wideband IT using three layers coupled line structure was proposed in [8]. However, these works also ignored the out-of-band suppression characteristics.

In this paper, the design method for the IT with high selectivity and wide out-of-band suppression characteristics is presented based on the series parallel coupled line and shunt transmission lines with characteristic impedance Z_1 and Z_2. To verify the proposed IT network, a 50-to-20 Ω IT was designed, simulated, and fabricated at a center frequency (f_0) of 2.6 GHz.

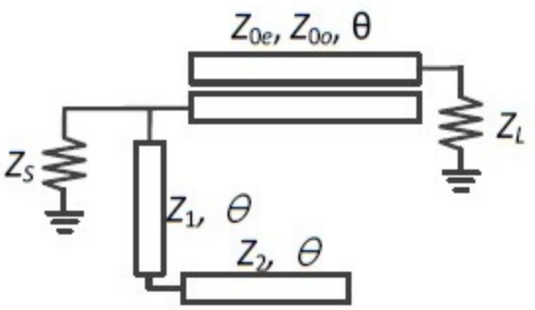

Fig. 1. Proposed structure of impedance transformer circuit.

II. Circuit Design

Fig. 1 shows the proposed structure of IT which transform a load impedance Z_L to a source impedance Z_S. It consists of an open-circuited coupled line and shunt stepped impedance transmission lines with the characteristic impedance Z_1 and Z_2. The electrical lengths of coupled line and shunt stepped impedance transmission lines are a quarter-wavelength (λ/4) and half-wavelength (λ/2) at f_0, respectively.

The return and transmission losses of the proposed IT network can be derived as (1) and (2) using the cascaded ABCD matrix.

$$S_{11} = \frac{ArZ_S + B - CrZ_S^2 - DZ_S}{ArZ_S + B + CrZ_S^2 + DZ_S} \tag{1}$$

$$S_{21} = \frac{2Z_S\sqrt{r}}{ArZ_S + B + CrZ_S^2 + DZ_S} \tag{2}$$

where

$$A = \frac{Z_p}{Z_m}\cos\theta \tag{3a}$$

$$B = j\frac{Z_m^2 - Z_p^2\cos^2\theta}{2Z_m\sin\theta} \tag{3b}$$

$$C = j\frac{1}{Z_m}\left(2\sin\theta - \frac{(Z_1+Z_2)Z_p}{\left(Z_1^2\tan\theta - Z_1Z_2\cot\theta\right)}\right) \tag{3c}$$

$$D = \frac{(Z_1+Z_2)\left(Z_m^2 - Z_p^2\cos^2\theta\right)}{2Z_m\sin\theta\left(Z_1^2\tan\theta - Z_1Z_2\cot\theta\right)} + \frac{Z_p}{Z_m}\cos\theta \tag{3d}$$

$$Z_p = Z_{0e} + Z_{0o} \tag{3e}$$

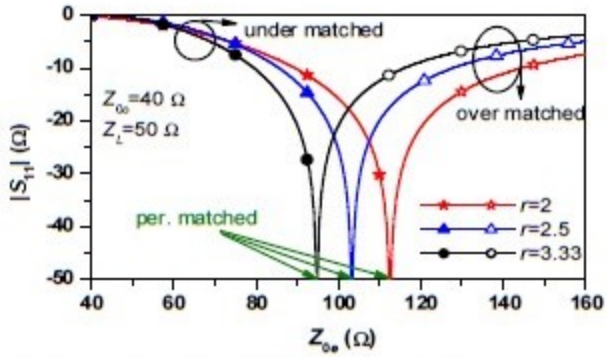

Fig. 2. Return loss characteristics at center frequency according to Z_{0e} with Z_L=50 Ω and r=2, 2.5, and 3.33.

$$Z_m = Z_{0e} - Z_{0o} \tag{3f}$$

$$\theta = \frac{\pi}{2}\frac{f}{f_0} \tag{3g}$$

$$r = \frac{Z_L}{Z_s} \tag{3h}$$

where f, r, Z_{0e}, and Z_{0o} are operating frequency, impedance transforming ratio, even-, and odd-mode impedances of coupled line, respectively. The return loss at f_0 can be obtained as (4).

$$S_{11}\big|_{f=f_0} = \frac{Z_m^2 - 4rZ_s^2}{Z_m^2 + 4rZ_s^2} \tag{4}$$

As seen from (4), the return loss only depends on Z_{0e} and Z_{0o} of the series coupled line. Therefore, Fig. 2 shows S_{11} characteristic at f_0 according to different values of Z_{0e} and r by assuming Z_{0o}=40 Ω and Z_L=50 Ω. From this figure, the three difference regions of S_{11} are categorized by (5).

$$(Z_{0e} - Z_{0o}) < 2Z_s\sqrt{r} \text{ : under-matched} \tag{5a}$$

$$(Z_{0e} - Z_{0o}) = 2Z_s\sqrt{r} \text{ : perfectly-matched} \tag{5b}$$

$$(Z_{0e} - Z_{0o}) > 2Z_s\sqrt{r} \text{ : over-matched} \tag{5c}$$

From these conditions, Z_{0e} with specified values of S_{11}, Z_s, and r at f_0 are obtained differently. For the under-matched condition, Z_{0e} is found as (6).

$$Z_{0e} = 2Z_S\sqrt{\frac{r\left(1 - S_{11}\big|_{f=f_0}\right)}{1 + S_{11}\big|_{f=f_0}}} + Z_{0o} \tag{6}$$

Similarly, Z_{0e} of the over-matched condition can be found as (7).

$$Z_{0e} = 2Z_S\sqrt{\frac{r\left(1 + S_{11}\big|_{f=f_0}\right)}{1 - S_{11}\big|_{f=f_0}}} + Z_{0o} \tag{7}$$

Since S_{11} is equal to zero in case of the perfectly matched condition, Z_{0e} is found as (8).

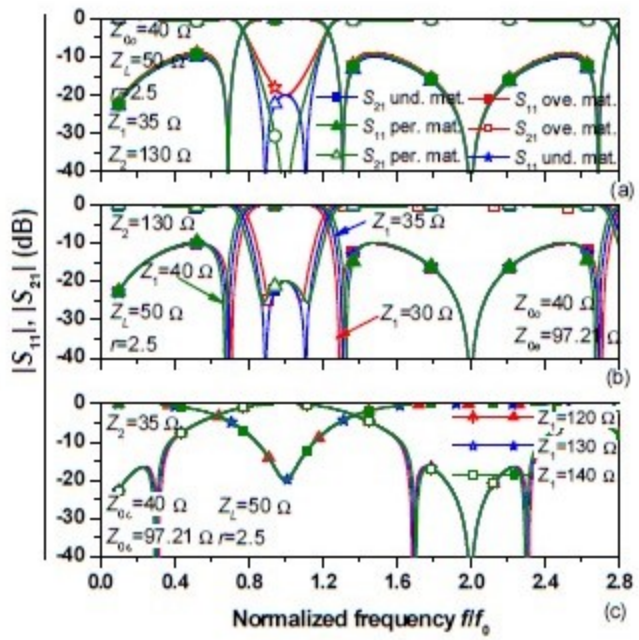

Fig. 3. Simulated S_{11} and S_{21} characteristics: (a) under-, perfect, and over-matched condition, (b) under-matched with variation of Z_1, and (c) under-matched in case of Z_1 higher than Z_2.

$$Z_{0e} = 2Z_S\sqrt{r} + Z_{0o} \tag{8}$$

Fig. 3(a) shows the S_{11} and S_{21} characteristics assuming the specific return loss. This simulation is performed by fixing the characteristic impedances of the shunt stepped impedance transmission lines as Z_1=35 Ω and Z_2=125 Ω and Z_{0e} are vary according to the matched conditions as (6) to (8), respectively. And impedance ratio of 2.5 is chosen. As seen from this figure, the under-matched condition shows the widest return loss bandwidth characteristic due to two transmission poles in the passband. Therefore, the under-matched condition is preferable for the frequency selective IT.

Fig. 3(b) shows the S-parameters characteristic of the under-matched condition according to different Z_1 assuming S_{11}=-20 dB at f_0. As Z_1 decreases, two transmission poles are closed in the passband, which provides relatively narrower bandwidth. Fig. 3(c) shows the S-parameters of the under-matched condition in case Z_1 is higher than Z_2. From the figure, two transmission zeros near the passband are moved far away from the passband and the frequency selective characteristics is worse. Therefore, the conditions of lower Z_1 and higher Z_2 are satisfied.

III. Simulation and Measurement

To validate the proposed IT, a 50-to-20 Ω (r=2.5) impedance transformer with the return loss of 20 dB at f_0= 2.6 GHz was designed, simulated, and measured. And the

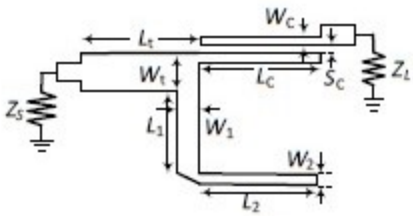

W_c=0.92 mm	L_c=18.9 mm
S_c=0.2 mm	L_t=20.5 mm
W_t=4.2 mm	L_1=19.65 mm
W_1=3.4 mm	L_2=19.05 mm
W_2=0.6 mm	

(a) (b)

Fig. 4. (a) EM simulation layout and (b) physical dimensions of the proposed impedance transformer.

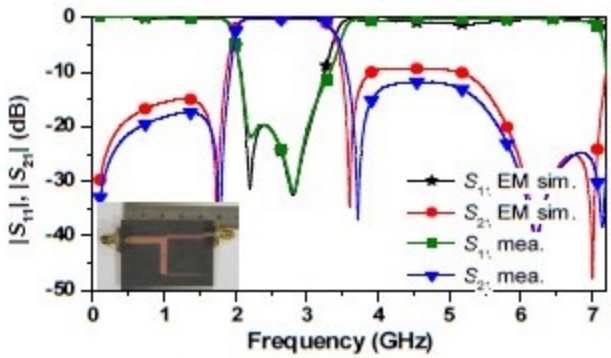

Fig. 5. EM simulation and measurement results.

under-matched condition was chosen. The circuit element values of design network were determined as Z_{0e} =97.21 Ω, Z_{0o}=40 Ω, Z_1=35 Ω, and Z_2=130 Ω, respectively. The circuit was fabricated on substrate RT/Duroid 5880 with a dielectric constant (ε_r) of 2.2 and a thickness (h) of 31 mils. The electromagnetic (EM) simulation was performed using HFSS v15 from Ansoft.

The EM simulation layout and its physical dimensions of the designed IT are shown in Fig. 4. A quarter-wavelength IT at the source port is used for the measurements with a 50 Ω termination network analyzer. The circuit size of the fabricated IT is 23 × 28 mm^2 (without a quarter-wavelength IT for the measurement).

Fig. 5 shows the EM simulation, measurement results, and the photograph of the fabricated IT. The measurement results agree with those of the EM simulations. From the measurement, the return loss is 22.8 dB at f_0=2.6 GHz. Similarly, the 20 dB return loss bandwidth is 0.8 GHz (2.2 - 3 GHz). The insertion loss in the passband (2.2 - 3 GHz) is smaller than 0.4 dB, including the loss of a quarter-wavelength IT for the measurement. As seen in measurement result, four transmission zeros at out-of-passband are obtained, which provides good out-of-band suppression characteristics. The shunt stepped impedance transmission line generates transmission-zeros at 1.77 GHz, 3.7 GHz, and 7.15 GHz, respectively. Similarly, the quarter-wavelength coupled line generates a transmission zero at 6.2 GHz. The out-of-band suppression is higher than 17 dB from DC to 1.85 GHz at the lower side of the passband, and higher than 11 dB from 3.5 GHz to 7.2 GHz at the upper side of passband. Therefore, the proposed IT provides high frequency-selectivity passband matching characteristics as well as wide out-of-band suppression. The high frequency selective characteristic of the proposed IT is beneficial to the frequency selective circuits design.

IV. Conclusion

This paper presents the design of an impedance transformer with high passband selective and wide out-of-band suppression characteristics by controlling the characteristic impedances of series coupled line and shunt stepped impedance transmission line stub. The proposed IT is simple to design and fabricate and is also expected to be applicable in various RF circuits and systems that require frequency selective performances.

References

[1] J. Lim, S. Oh, J. Koo, Y. Jeong, and D. Ahn, "A power divider with adjustable dividing ratio," *IEICE Trans. Electron.*, vol. E91-C, no. 3, pp. 389–391, Mar. 2008.

[2] L. Lee, H. Youn, and M. F. Iskander, "Long slot array (LSA) antenna integrated with compact broadband coupled microstrip impedance transformer," *Antennas Propaga. Society Interna. Symposium*, pp. 1-2, 2012.

[3] H. Ahn and T. Itoh, "New isolation circuits of compact impedance-transforming 3-dB baluns for theoretically perfect isolation and matching," *IEEE Trans. Microw. Theory Techn.*, vol. 58, no. 12, pp. 3892–3902, Dec. 2010.

[4] H. Choi, S. Shim, Y. Jeong, J. Lim, and C. Kim, "A compact DGS load-network for highly efficient class-E power amplifier," *Proceeding 39th European Microw. Confer.*, pp. 492–495, 2009.

[5] H. Ahn and T. Itoh, "Impedance-transforming symmetric and asymmetric and asymmetric DC blocks," *IEEE Trans. Microw. Theory Techn.*, vol. 58, no. 9, pp. 2463–2474, Sep. 2010.

[6] K. Ang, C. Lee, and Y. Leong, "Analysis and design of coupled line impedance transformers," *Interna. Microw. Sympo. Digest*, vol. 3, pp. 1951-1954, 2004.

[7] J. Cheng, E. Li, and Y. Huang, "Designs of bandwidth-controllable impedance transformers using dual transmission lines," *Electronics Lett.* vol. 48, no. 15, pp. 931-932, 2012.

[8] H. Nguyen, K. Ang, and G. Ng, "Design of coupled three-line impedance transformers," *IEEE Microw. Wireless Compon. Lett.*, vol. 24, no. 2, pp. 84–86, Feb. 2014.